STM JOURNALS

Journal of
Polymer & Composites

https://journals.stmjournals.com/jopc

ISSN: 2321-2810 (Online)
ISSN: 2321-8525 (Print)
Volume 14, Special Issue 4, 2026
January–December
DOI (Journal): 10.37591/JoPC

Research JoPC

In-Situ Polymerized GO/PANI Composites: Structural Evolution, Optical Modulation, and NH_3 Sensing at Room Temperature

Shahebaz S. Khan[1], Shaikh Mohd. Waseem[1], Nikeshkumar N. Ingle[2], Kranti Zakde[3,*]

Abstract

Graphene oxide (GO)/polyaniline (PANI) composites with varying PANI contents (20, 40, and 60 wt%) were synthesized via in-situ oxidative polymerization and systematically investigated for their structural, morphological, optical, and gas-sensing properties. X-ray diffraction (XRD) confirmed a progressive increase in interlayer spacing and partial exfoliation of GO layers with increasing PANI content, indicating intercalation-assisted hybridization. Fourier transform infrared (FTIR) spectroscopy revealed the characteristic vibrational bands of both constituents and confirmed strong interfacial interactions through hydrogen bonding and π–π stacking. Scanning electron microscopy (SEM) showed a morphological evolution from wrinkled GO sheets to a densely interconnected composite network, most pronounced for the GO/PANI–40 composition. UV–Visible spectroscopy and Tauc analysis demonstrated enhanced electronic delocalization and a systematic reduction in optical band gap from 3.10 eV for pristine GO to 2.55 eV for GO/PANI–60, reflecting extended conjugation across the GO–PANI interface. The room-temperature ammonia (NH_3) sensing performance was evaluated for all compositions. The GO/PANI–40 composite exhibited the optimal response, combining high sensitivity, rapid response–recovery kinetics (response time ≈ 35 s and recovery time ≈ 50 s), excellent selectivity toward NH_3 over interfering gases, good repeatability over successive cycles, and long-term stability retaining more than 95% of its initial response over 30 days. This superior behaviour is attributed to synergistic interfacial charge transfer, abundant adsorption sites, and efficient charge-transport pathways within the hybrid network, highlighting GO/PANI composites as promising candidates for reliable room-temperature NH_3 detection.

Keywords: GO/PANI composite, NH_3 sensing, XRD, IR, SEM

***Author for Correspondence**
Kranti Zakde
E-mail: kzakde@mgmu.ac.in

[1]Research Scholor, Department of Physics, School of Basic and Applied Sciences, MGM University, Chhatrapati Sambhaji Nagar, Maharashtra, India
[2]Assistant Professor, Department of Physics, School of Basic and Applied Sciences, MGM University, Chhatrapati Sambhaji Nagar, Maharashtra, India
[3]Associate Professor, Department of Physics, School of Basic and Applied Sciences, MGM University, Chhatrapati Sambhaji Nagar, Maharashtra, India

Received Date: July 06, 2026
Accepted Date: July 28, 2026
Published Date: August 14, 2026

Citation: Shahebaz S. Khan, Shaikh Mohd. Waseem, Nikeshkumar N. Ingle, Kranti Zakde. In-Situ Polymerized GO/PANI Composites: Structural Evolution, Optical Modulation, and NH_3 Sensing at Room Temperature. Journal of Polymer & Composites. 2026; 14(Special Issue 4): S509–S525p.

INTRODUCTION

In the recent years, the monitoring of poisonous and harmful gases in trace concentration has attracted more attentions due to their detrimental effects on public health, environmental quality governance and industrial security. Of these gases in the air, ammonia (NH_3) is an important substance because it has been widely used for fertilizer production and preservation of food as well as chemical manufacturing, although its high exposure was known to cause damage [1]. Traditional gas sensors prepared with metal oxides (e.g., SnO_2, ZnO, and WO_3) generally must be operated at high temperature so that they can achieve relatively high sensitivity by way of sacrificing power consumption or operation stability. Therefore, recently, much attention has been paid on the exploration of alternative sensing materials that can work well at

room temperature with excellent performance (high sensitivity, good selectivity), fast response–recovery behaviour as well as long-term stability [2].

Tunable electrical conductivity, chemical versatility and ease of synthesis have led conducting polymers to become promising materials for room-temperature gas sensing. Among the available conducting polymers, polyaniline (PANI) is one of the most sought after owing to its environmental stability, reversible redox behaviour and protonation–deprotonation characteristics that enable successful interaction with oxidising as well as reducing gases [3]. Nevertheless, typical pure PANI based systems are characterized by weak mechanical strength lack of surface area and slow recovery kinetics in gas sensing process, making the performance applicable to a stand-alone gas sensor impractical. To surpass these disadvantages, much attention has been devoted to hybrid composites by incorporation of conducting polymers (CPs) with carbon-based nanomaterials that can improve its surface activity, conductivity and charge transfer pathways [4].

Graphene oxide (GO, the chemically modified form of graphene) with two-dimensional layered structure has many oxygen-containing functional groups like hydroxyl, epoxy and carboxyl groups [5]. These functionalities make GO hydrophilic and easily dispersed in water, as well as active sites for chemical bonding with polymeric residues. In addition, GO possesses large specific surface area, mechanical strength and electro-conductive character is an ideal support material for polymer PC. GO, when combined with conducting polymers (i.e., PANI), can serve as a suitable template to facilitate uniform polymer growth and to achieve better interfacial interaction and enhanced electrical performance along with sensing characteristics [6].

It has been reported that GO/PANI composites have better gas-sensing properties than the single component because of some synergistic effect between each other. The oxygen–containing groups of GO have strong interactions with the nitrogen sites of PANI in hydrogen bonding between them or in the form of electrostatic attractions, then achieving charge transfer across the interface. This results in high EM, large active surface and good gas molecules adsorption–desorption kinetics [7]. However, the sensing properties of these composites strongly depend on the ratio of GO to PANI as they control the morphology, crystallization and electronic coupling at the interface in hybrid structures. However, an informative insight into the relationship between composition, structural evolution and gas-sensitive property helps to optimize these materials for practical applications.

In this study, graphene oxide–polyaniline (GO/PANI) composites with various PANI loadings (20 wt%, 40 wt% and 60 wt%) were synthesized by in-situ oxidative polymerization. The structural, morphological and optical changes caused as a function of PANI content have been sought to be explained with relation to the room-temperature gas-sensing behavior toward ammonia of the composites. The phase composition, chemical bonding, surface morphology and optical properties were studied by X-ray diffraction (XRD), Fourier transform infrared (FTIR) spectroscopy, scanning electron microscopy (SEM), and UV–Visible spectroscopy. Response, selectivity, response–recovery time, repeatability and stability were investigated by gas-sensing experiments. The results indicate that GO/PANI-40 not only has synergistic effects of the two individual materials but also can promote interfacial contact between GO and PANI, which is beneficial for charge transfer performance, as well as superior sensitivity performance, showing toward room temperature detection of ammonia.

EXPERIMENTAL

Materials

Graphite powder (99.5%, <45 μm), sulfuric acid (H_2SO_4, 98%), potassium permanganate ($KMnO_4$, 99%), hydrogen peroxide (H_2O_2, 30%), aniline monomer ($C_6H_5NH_2$, 99.5%), and ammonium persulfate [$(NH_4)_2S_2O_8$] APS – 98%) were purchased from Merck and used as-received without further purification. The washing and dispersion of CQDs were conducted with deionized (DI) water.

Synthesis of Graphene Oxide (GO)

Graphene oxide was prepared by modified Hummers' method. Typical procedure: 2 g of graphite powder was added to 46 mL concentrated H_2SO_4 with continuous stirring at ice-bath temperature (≤10°C); then, a fine slurry consisting of 6 g $KMnO_4$ was slowly introduced into the flask over time to prevent overheating. The resulting reaction mixture was stirred for 2 h, and then 92 mL of DI water was slowly added drop by drop at a rate of 1.5/ h with temperature rising to 35°C. This product was further stirred for another hour at 80°C to make sure that graphite oxidation proceeded completely. Afterwards, 10 mL of 30% H_2O_2 was added to stop the reaction and its color became yellow. The resultant slurry was washed several times by 5% HCl and DI-H_2O until the pH of washing water reached neutral. The as-obtained product was vacuum dried at 60°C for 24 h to achieve fine brown color GO powder.

Synthesis of Polyaniline (PANI)

Polyaniline was synthesized by the chemical oxidative polymerization of aniline monomer. In a general procedure, 0.1 mol of aniline was dissolved in 100 mL of 1 M HCl with stirring to give a homogeneous solution. An oxidant solution was separately prepared by dissolving 0.1 mol of APS in HCl (100 mL, 1 M) and the resultant mixture was dropwise added to the aniline solution at 0–5 °C under vigorous stirring. The polymerization was carried out for 6h in an ice bath to ensure the full oxidation of monomer. The dark green precipitate of polyaniline (emeraldine salt) obtained was filtered, washed thoroughly with DI water and ethanol to remove any residual oxidant and oligomers, respectively, followed by drying under vacuum at 60°C for 24 h.

Preparation of GO/PANI Composites

The GO/PANI composites were fabricated by the in-situ polymerization method of aniline over GO suspension. Various fixed quantities of GO were sonicated in 1 M HCl for 1 h to achieve stable colloidal suspensions. Subsequently, aniline monomer was added to the GO suspension at varying weight ratios in CH_3COOH-HCl solution with different GO:PANI mass fractions, including GO/PANI-20, GO/PANI-40 and GO/PANI-60 (representing 20%, 40%, and 60 wt% of PANI). The reaction mixture was continuously stirred and the APS oxidant solution (aniline:APS molar ratio = 1:1) dropwise added at 0–5°C, and the polymerization continued for 6 h; the resulting composite precipitates with dark color were then filtered off and washed repeatedly using DI water and ethanol until neutral pH. The GO/PANI composites were then vacuum-dried at 60°C for 24 h and milled into the power form for characterization.

RESULTS AND DISCUSSION

X-Ray Diffraction (XRD) Analysis

X-ray diffraction was employed to investigate the structural evolution of GO, PANI, and GO/PANI composites containing 20, 40, and 60 wt% PANI. Measurements were performed using Cu Kα radiation (λ = 1.5406 Å, 40 kV, 30 mA), with diffraction data collected over the 2θ range of 5°–60° at a step size of 0.02°. The corresponding diffraction patterns are presented in Figure 1.

Pristine GO exhibits a characteristic diffraction peak at 2θ = 11.3°, indexed to the (001) plane. Based on Bragg's law [8], the calculated interlayer spacing is 0.78 nm, which reflects the incorporation of oxygen-containing functional groups and intercalated water molecules between graphene layers. A weak reflection at 2θ = 26.6°, corresponding to the (002) plane with d_{002} = 0.34 nm, arises from residual graphitic domains that retain partial structural order. An additional weak peak observed at 2θ = 42.4° is assigned to the (100) plane and is associated with the in-plane periodicity of sp^2-hybridized carbon atoms. Overall, the diffraction pattern of GO indicates partial lamellar ordering accompanied by significant structural disorder induced by oxidation.

The XRD pattern of pure PANI (emeraldine salt) displays broad diffraction peaks at 2θ = 9.1°, 15.0°, 20.7°, and 25.3°, which can be indexed to the (020), (011), and (200) planes [6]. These broad features indicate the semi-crystalline nature of PANI, characterized by short-range order and partially aligned polymer chains embedded in an amorphous matrix. The diffuse halo in the 2θ range of 18°–26° further

confirms the coexistence of crystalline and amorphous phases, consistent with chemically synthesized conducting polymers.

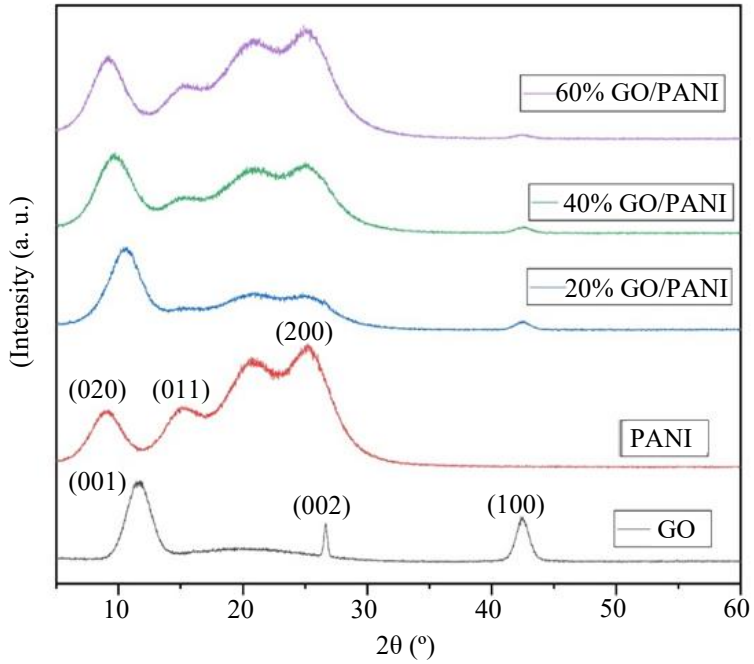

Figure 1. XRD patterns of GO, PANI, and GO/PANI composites (20, 40, 60 wt% PANI).

Upon incorporation of 20 wt% PANI, the GO/PANI composite exhibits a noticeable shift of the GO (001) reflection from 2θ = 11.3° to 10.6°, corresponding to an increased interlayer spacing of d_{001} = 0.84 nm. This expansion suggests partial intercalation of PANI chains into the GO interlayer galleries. The enhanced broad halo observed in the 2θ range of 20°–27° compared to pristine GO indicates increased structural disorder and partial exfoliation of GO layers due to polymer insertion and interfacial interactions.

For the composite containing 40 wt% PANI, the GO (001) peak further shifts toward lower diffraction angles, reflecting continued interlayer expansion and improved polymer intercalation. Simultaneously, the intensity of the GO (002) reflection markedly decreases, indicating disruption of long-range lamellar stacking. The pronounced broadening of the diffraction band in the range of $20° \leq 2\theta \leq 27°$ suggests an increased degree of amorphization, consistent with the formation of a disordered hybrid network in which GO layers are partially exfoliated and uniformly dispersed within the PANI matrix.

In the GO/PANI composite with 60 wt% PANI, the diffraction pattern is dominated by polymer-related features, indicating substantial structural modification of GO. The (001) reflection appears at 2θ = 9.25°, corresponding to a maximum interlayer spacing of d_{001} = 0.96 nm. The near disappearance of the GO (002) and (100) reflections at 26.6° and 42.4°, respectively, confirms extensive exfoliation of GO sheets and their homogeneous distribution within the polymer matrix. The broad diffraction band in the 2θ range of 20°–27° signifies a predominantly amorphous structure, demonstrating the effective destruction of the original layered GO architecture.

The systematic shift of the GO (001) peak from 2θ = 11.3° (d = 0.78 nm) for pristine GO to 2θ = 9.25° (d = 0.96 nm) for GO/PANI-60 clearly indicates a progressive increase in interlayer spacing with increasing PANI content [9]. This structural evolution is attributed to the gradual intercalation of PANI chains between GO layers, facilitated by strong interfacial interactions such as hydrogen bonding and electrostatic attraction. The concurrent reduction in long-range crystallinity and enhancement of amorphous character confirm that GO/PANI nanocomposites are formed through intercalation-assisted

partial exfoliation, resulting in structurally disordered hybrids with improved interfacial compatibility and molecular-level homogeneity [10].

Fourier Transform Infrared (FTIR) Spectroscopy Analysis

The FTIR spectra of pristine PANI and GO–PANI nanocomposites containing 20, 40, and 60 wt% GO are presented in Figure 2. All spectra display characteristic vibrational bands associated with the functional groups of both graphene oxide (GO) and polyaniline (PANI), confirming the successful formation of the composite structures [11].

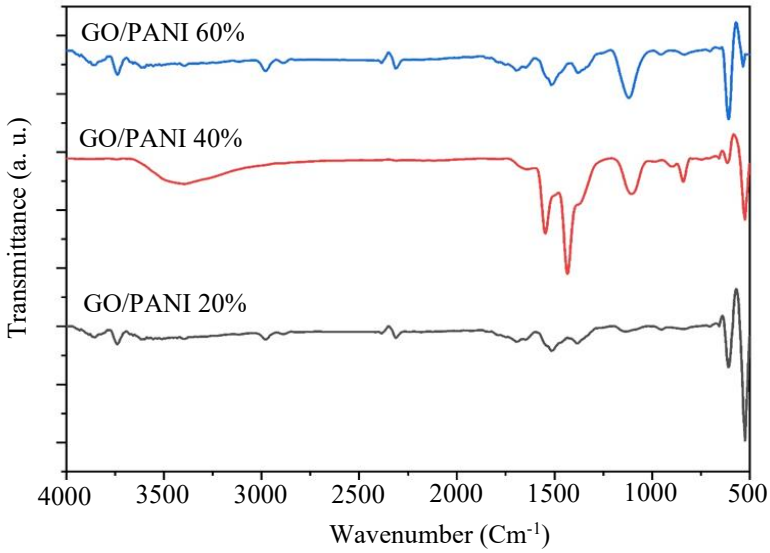

Figure 2. FTIR spectra of GO, PANI, and GO/PANI composites showing interfacial bonding and chemical interaction.

A broad absorption band centered around 3400 cm^{-1} is observed in all samples, which arises from the overlapping O–H and N–H stretching vibrations. The intensity and breadth of this band increase with higher GO content, indicating enhanced hydrogen bonding interactions originating from oxygen-containing functional groups on GO sheets. The absorption band near 2920 cm^{-1} is assigned to C–H stretching vibrations of aliphatic groups.

A prominent absorption band around 1720 cm^{-1} becomes increasingly pronounced with increasing GO content, particularly in the GO–PANI 60% composite. This band corresponds to the C=O stretching vibration of carboxylic groups present in GO, confirming its effective incorporation within the PANI matrix. The characteristic bands of PANI appear at 1560 cm^{-1} and 1480 cm^{-1}, corresponding to the C=C stretching vibrations of the quinoid and benzenoid rings, respectively. The relative intensity ratio of these bands (I_{1560}/I_{1480}) reflects the oxidation state of PANI and suggests partial charge delocalization along the polymer backbone due to interaction with GO.

The absorption band in the range of 1290–1220 cm^{-1} is attributed to C–N stretching vibrations of the benzenoid amine units, while the peak near 1140 cm^{-1} corresponds to the $B–NH^{+}=Q$ vibration, which is considered a characteristic fingerprint of the conductive emeraldine salt form of PANI. Additional bands observed at 1030–1025 cm^{-1} are associated with C–O stretching vibrations, whereas the band at 793 cm^{-1} is assigned to C–H out-of-plane bending modes.

The systematic enhancement of oxygen-related vibrational bands (C=O, C–O, and O–H) with increasing GO content indicates strong interfacial interactions between GO sheets and PANI chains, likely involving hydrogen bonding and π–π stacking. These interactions suggest that GO acts not only as a structural support but also promotes effective interfacial coupling, which is beneficial for charge transport within the composite network.

FTIR analysis confirms the successful synthesis of GO–PANI nanocomposites and the presence of strong interfacial interactions between GO and the conducting polymer. Such interactions are expected to play a critical role in enhancing the electrical and sensing performance of the composite materials [12].

SEM Analysis

The surface morphology and microstructural characteristics of graphene oxide (GO), polyaniline (PANI), and GO/PANI composites with PANI content of 20%, 40%, or 60% were examined using scanning electron microscopy (SEM). Pristine GO manifests a thin, wrinkled, sheet-like morphology with obvious folds and crumples – the appearance of exfoliated graphene oxide layers. This highly wrinkled surface arises from the introduction of oxygen-containing functional groups such as hydroxyl, epoxy, and carboxyl moieties. These distort the planar sp^2 carbon network, increase the roughness of surface area as well as layer distance. Representative micrographs of this morphological evolution are presented in Figure 3.

On the other hand, pure PANI has an agglomerated granular and fibrillar morphology made of interconnected polymer chains forming irregular clusters. This microstructural feature is typical of PANI synthesized by oxidative polymerization, and represents a porous, uneven surface with limited long-range order [13].

For the GO/PANI composite with 20 wt% PANI content, SEM photographs reveal that PANI particles are uniformly anchored to the GO sheets, only partially covering lamellar surfaces and forming a continuous sash. GO sheets act as very effective nucleation sites, for the growth and deposition of PANI chains. Through interfacial interactions between the amine group of PANI and the oxygenated functional group of GO, PANI grows on GO. As a result, a heterogeneous but well-integrated morphology is observed, where the granular features of PANI are intimately associated with the wrinkled GO framework.

With an increase in PANI to 40 wt%, the GO sheets are covered more densely. The layered morphology becomes gradually less distinct. Forming interconnected polymer networks that bond adjacent GO sheets together creates a more compact microstructure with reduced void space and greater interfacial contact. This indicates strong physical adhesion and improved compatibility between GO and PANI components.

At a higher PANI loading of 60 wt%, SEM micrographs show that GO sheets are almost completely encased within the PANI matrix. A continuous polymeric surface becomes dense and regular. The characteristic texture of GO is largely blanked out, indicating a high degree of coverage and strong interfacial bonding. An irregular, but compact, morphology suggests that GO is effectively dispersed within the conductive polymer framework. Successful nano-scale hybridization.

Taken together, the progressive morphological evolution from wrinkled GO sheets to a densely interconnected GO/PANI composite structure confirms the effective integration of PANI into the GO matrix. Such a uniform and interconnected microstructure is expected to promote improved charge transport, greater mechanical stability, and efficient pathways for the interaction of different substances – properties that are critical for high-performance, multi-functional GO/PANI hybrid materials [14].

UV–Visible Spectroscopy Analysis

The optical properties and electronic interactions of graphene oxide (GO), polyaniline (PANI), and GO/PANI composites containing 20, 40, and 60 wt% PANI were investigated using UV–Visible spectroscopy over the wavelength range of 200–800 nm. The absorption spectrum of pristine GO exhibits a strong band at 231 nm, which is attributed to π–π^* electronic transitions within the conjugated C=C bonds of aromatic carbon domains [15]. A weak shoulder observed near 303 nm corresponds to n–π^* transitions associated with carbonyl (C=O) groups, confirming the presence of oxygen-containing functional groups introduced during graphite oxidation. These spectral features indicate that the electronic structure of GO consists of isolated sp^2 carbon domains separated by oxygen-rich regions, resulting in disrupted conjugation. The corresponding absorption spectra are shown in Figure 4.

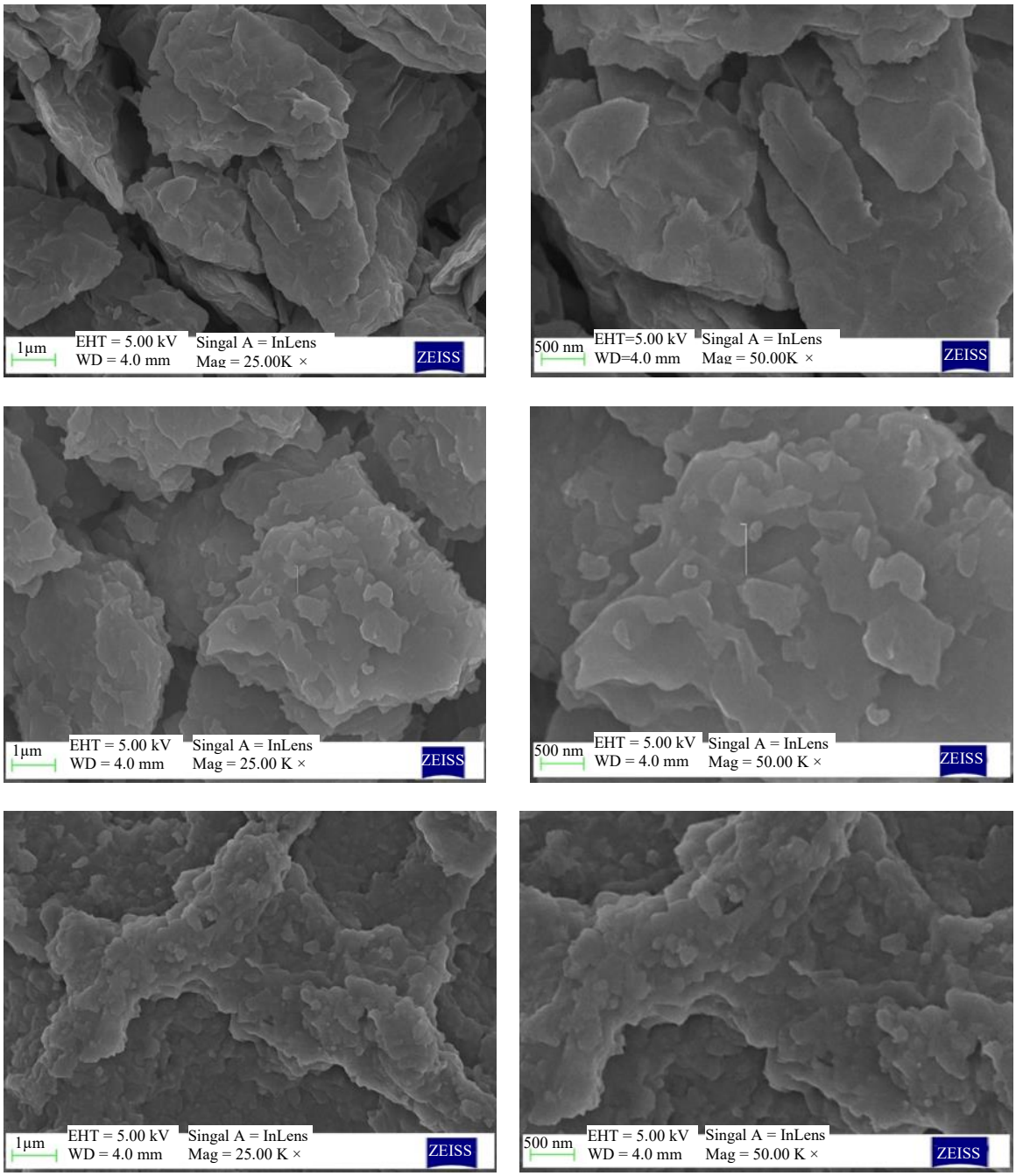

Figure 3. SEM micrographs of (a) GO, (b) PANI, and GO/PANI composites with 20, 40, and 60 wt% PANI.

Pure PANI in the emeraldine salt form exhibits two characteristic absorption bands centered at 327 nm and 624 nm. The band at 327 nm is associated with π–π* transitions within the benzenoid segments of the polymer backbone, while the absorption at 624 nm arises from polaron-related transitions along the conjugated polymer chain. An additional weak band observed near 430 nm is attributed to transitions between benzenoid and quinoid units, confirming the coexistence of oxidized and reduced segments typical of the emeraldine state. These spectral characteristics reflect the semi-crystalline nature and conductive behavior of PANI.

For the GO/PANI composite containing 20 wt% PANI, the absorption spectrum closely resembles that of pure PANI but exhibits noticeable red shifts. The characteristic GO absorption edge shifts from 231 nm to 238 nm, indicating enhanced electronic delocalization due to interfacial interaction between

GO sheets and PANI chains. Simultaneously, the PANI-related absorption bands become more intense, suggesting improved charge transfer between oxygenated functional groups of GO and nitrogen-containing moieties of PANI. These changes imply partial reduction of GO during in-situ polymerization and the formation of extended conjugation across the GO–PANI interface.

In the GO/PANI-40 composite, absorption peaks are observed at 242 nm and 636 nm, accompanied by significant broadening in the visible region. This behavior indicates increased conjugation length and stronger electronic coupling between GO and PANI. The enhanced absorbance intensity across the visible range reflects improved electronic delocalization and the development of efficient charge transport pathways within the composite network.

At a higher PANI loading of 60 wt%, the absorption spectrum is dominated by polymer-related bands located at 246 nm and 650 nm, while the GO-associated features become indistinct. The pronounced red shift and increased band intensity suggest higher charge carrier mobility and stronger interfacial interaction between PANI chains and GO layers. The suppression of GO-specific absorption features indicates extensive coverage of GO sheets by the polymer matrix, resulting in a unified optoelectronic response.

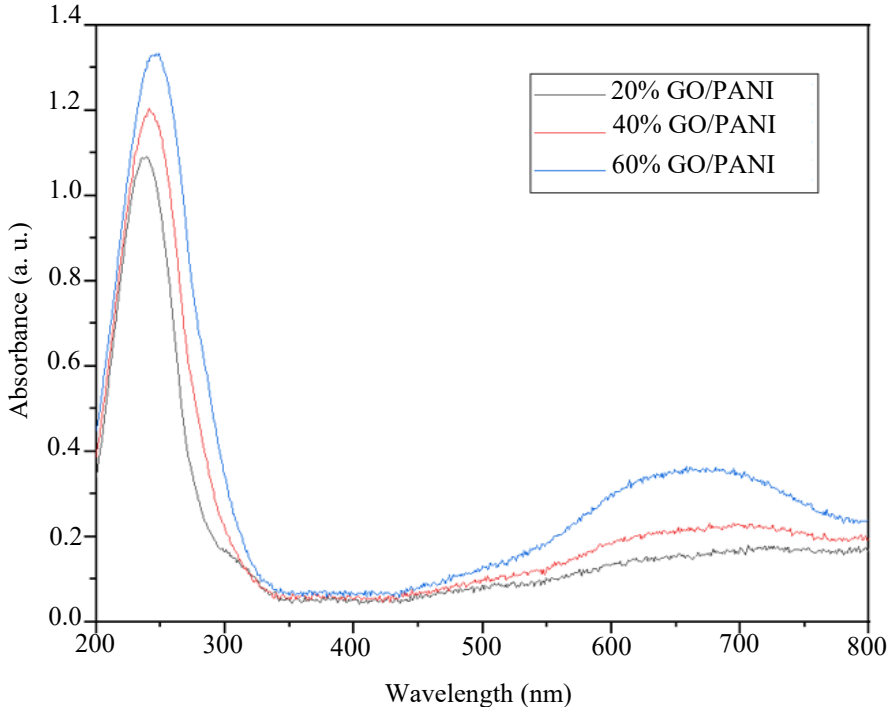

Figure 4. UV–Vis absorption spectra of GO, PANI, and GO/PANI composites (band shift and intensity variation).

The systematic red shift of absorption bands with increasing PANI content indicates a progressive reduction in optical band gap energy, arising from enhanced π-electron delocalization and the formation of a continuous conjugated network within the composites. Overall, UV–Visible analysis confirms that incorporation of GO into the PANI framework significantly enhances light absorption and electronic transport properties through strong interfacial coupling and extended conjugation. These attributes highlight the potential of GO/PANI composites for advanced optoelectronic and sensing applications.

Optical band gaps (E_g) were estimated using Tauc analysis based on the relation [15]:

$$(\alpha h\nu)^n = C(h\nu - E_g)$$

where α is the absorption coefficient, hν is the photon energy, C is a proportionality constant, and n depends on the nature of the optical transition (n = 2 for direct allowed transitions and n = 1/2 for indirect allowed transitions). For transmission measurements, the absorption coefficient was calculated from absorbance (A) using the relation α = 2.303A/L, where L is the optical path length (1 cm). For diffuse reflectance spectra, the Kubelka–Munk function [16],

$$F(R) = (1 - R)^2/2R,$$

was employed as a surrogate for α.

Tauc plots were constructed as $(\alpha h\nu)^{1/2}$ versus hν for the indirect allowed transition model and $(\alpha h\nu)^2$ versus hν for the direct allowed model [17]. Linear regions near the absorption edge were identified by maximizing the coefficient of determination (R^2) over contiguous fitting windows, and the optical band gap was determined from the intercept of the best-fitting linear region with the energy axis. For all samples, the indirect allowed representation exhibited a broader linear fitting range with higher R^2 values; therefore, indirect optical band gaps are reported.

The extracted band-gap values show a monotonic decrease with increasing PANI content, consistent with the red shift observed in the UV–Visible spectra and the progressive enhancement of electronic coupling at the GO–PANI interface. The optical band gap of pristine graphene oxide was determined to be 3.10 eV, reflecting its disrupted π-conjugated structure caused by extensive oxidation. Pure polyaniline in the emeraldine salt form exhibits a lower band gap of 2.85 eV, which is associated with its partially conjugated polymer backbone and intrinsic charge delocalization. Upon incorporation of PANI into the GO matrix, a progressive reduction in band gap is observed. The GO/PANI composite containing 20 wt% PANI shows an optical band gap of 2.72 eV, indicating the onset of interfacial electronic coupling between GO sheets and polymer chains. With further increase in PANI content, the band gap decreases to 2.63 eV for the GO/PANI–40 wt% composite, suggesting enhanced conjugation and charge transfer interactions. At the highest PANI loading of 60 wt%, the GO/PANI composite exhibits the lowest band gap of 2.55 eV, confirming strong interfacial hybridization and effective extension of the conjugated network within the composite system. The Tauc plots used to obtain these band-gap values are presented in Figure 5.

These results demonstrate a systematic band-gap narrowing of up to $\Delta E_g \approx 0.55$ eV from pristine GO to the GO/PANI–60 wt% composite. This trend correlates well with the structural and spectroscopic observations from XRD and FTIR analyses. The reduction in band-gap energy is attributed to enhanced interfacial charge-transfer interactions, increased π–π conjugation, and partial restoration of sp^2 domains within GO during in-situ polymerization of PANI. Collectively, these effects promote greater carrier delocalization, lower optical transition energies, and strengthened sub-bandgap absorption in the GO/PANI hybrid system.

Gas Sensing Study

The gas-sensing performance of graphene oxide (GO), polyaniline (PANI), and GO/PANI composites containing 20, 40, and 60 wt% PANI was systematically evaluated toward ammonia (NH_3) at ambient temperature. Thin films of the sensing materials were prepared by dispersing the powders in N-methyl-2-pyrrolidone, followed by drop-casting onto interdigitated gold electrodes and drying at 60°C for 12 h to ensure uniform film formation and good adhesion. The electrical resistance of each sensor was measured under dry air and upon exposure to controlled concentrations of NH_3 using a gas-flow chamber coupled with a digital electrometer. The sensing response (S) was calculated using the relation [18]:

$$S = \frac{R_a - R_g}{R_g} \times 100$$

where R_a and R_g represent the sensor resistance in air and in the presence of the target gas, respectively.

This study emphasizes the relationship between microstructural features, interfacial interactions, and gas-sensing performance as a function of PANI content in the composite system.

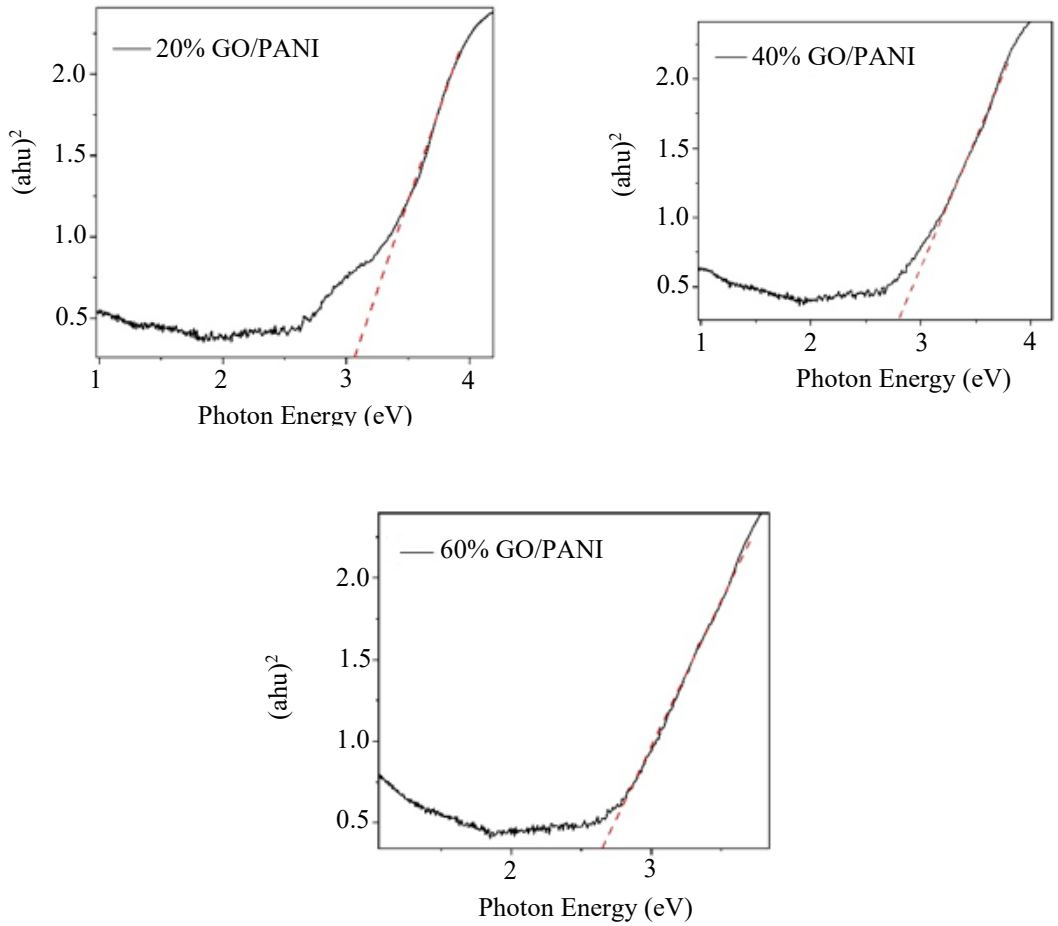

Figure 5. Tauc plots $(\alpha h\nu)^{1/2}$ vs. hν for estimation of optical band gaps of GO, PANI, and composites.

Gas Sensing Mechanism

The NH_3 sensing mechanism of the GO/PANI composite is governed by a reversible charge-transfer interaction between gas molecules and the surface of the sensing layer. PANI, being a p-type conducting polymer, contains protonated amine (–NH–) and imine (=N–) groups that act as active adsorption sites. Upon exposure to NH_3, an electron-donating reducing gas, NH_3 molecules interact with these protonated nitrogen sites, resulting in partial deprotonation of the PANI chains. This process decreases hole carrier concentration, leading to an increase in the electrical resistance of the sensor.

GO plays a complementary role by providing a large specific surface area, abundant oxygen-containing functional groups, and efficient charge transport pathways. The hydroxyl and epoxy functionalities on GO facilitate hydrogen bonding and dipole–dipole interactions with NH_3 molecules, thereby enhancing gas adsorption and sensitivity. In addition, GO sheets promote rapid charge redistribution across the GO–PANI interface, improving response kinetics.

Upon removal of NH_3, desorption occurs, and the sensor resistance gradually recovers to its initial value, confirming the reversible nature of the sensing process. The overall gas-sensing mechanism involves adsorption, charge transfer, and desorption of NH_3 molecules at the GO/PANI interface, as schematically illustrated, highlighting the synergistic interaction between GO and PANI that enables efficient charge modulation and accelerated response–recovery behaviour [19]. This adsorption–charge-transfer–desorption process is illustrated schematically in Figure 6.

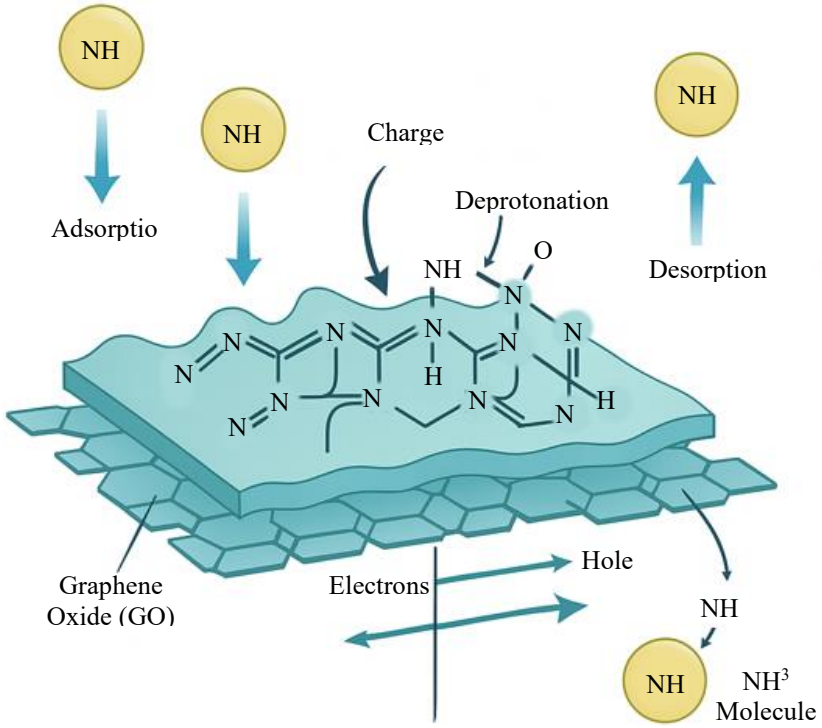

Figure 6. Schematic representation of the gas-sensing mechanism of GO/PANI composite sensor showing NH_3 adsorption and charge transfer.

Selectivity Analysis

Selectivity is a critical requirement for practical gas sensors, as it determines the ability of a sensing material to discriminate the target gas from interfering species. The selectivity performance of GO/PANI composites was evaluated by exposing the sensors to NH_3, CO, H_2, CH_4, and ethanol vapors at a fixed concentration of 100 ppm under identical experimental conditions. Among the investigated compositions, the GO/PANI–40 wt% composite exhibited the highest sensing response toward NH_3 while showing negligible responses to the other tested gases, as illustrated by the comparative response percentages presented in Figure 7.

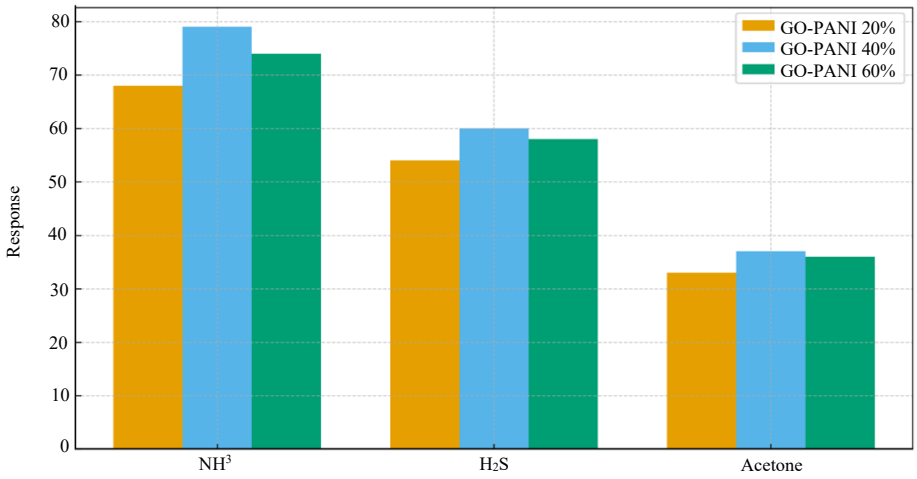

Figure 7. Gas selectivity response of GO/PANI composites toward different test gases (NH_3, CO, H_2, CH_4, and ethanol) at 100 ppm.

The superior selectivity toward NH_3 is primarily attributed to the strong acid–base interaction between NH_3 molecules, which act as Lewis bases, and the protonated nitrogen sites ($–NH^+–$) of PANI, which

function as Lewis acid centers. This interaction induces reversible deprotonation of the PANI backbone, resulting in a pronounced modulation of charge carrier concentration and, consequently, a significant change in sensor resistance. In contrast, nonpolar gases, such as H_2 and CH_4, as well as weakly interacting species, like CO and ethanol, do not produce comparable charge-transfer interactions, leading to substantially lower sensor responses.

The incorporation of GO further enhances selectivity by providing a large specific surface area and abundant oxygen-containing functional groups that preferentially interact with polar NH_3 molecules through hydrogen bonding and dipole–dipole interactions. The synergistic contribution of electrostatic adsorption on GO sheets and chemical interaction with the PANI chains results in a highly selective sensing behavior. The response profile summarized in Figure 7 clearly demonstrates the dominant sensitivity of the GO/PANI composite toward NH_3 at 100 ppm, confirming the effectiveness of the hybrid material for selective ammonia detection [9].

Gas Response as a Function of Concentration

To evaluate the quantitative sensing performance, the response of GO/PANI composite sensors was investigated over NH_3 concentrations ranging from 10 to 200 ppm. The sensing response increases monotonically with increasing NH_3 concentration and begins to approach saturation beyond 150 ppm, indicating progressive occupation and eventual saturation of available surface adsorption sites. Among the investigated compositions, the GO/PANI–40 wt% composite exhibits the highest response magnitude and the best linearity within the low-concentration regime of 10–100 ppm, as evident from the response–concentration relationship shown in Figure 8.

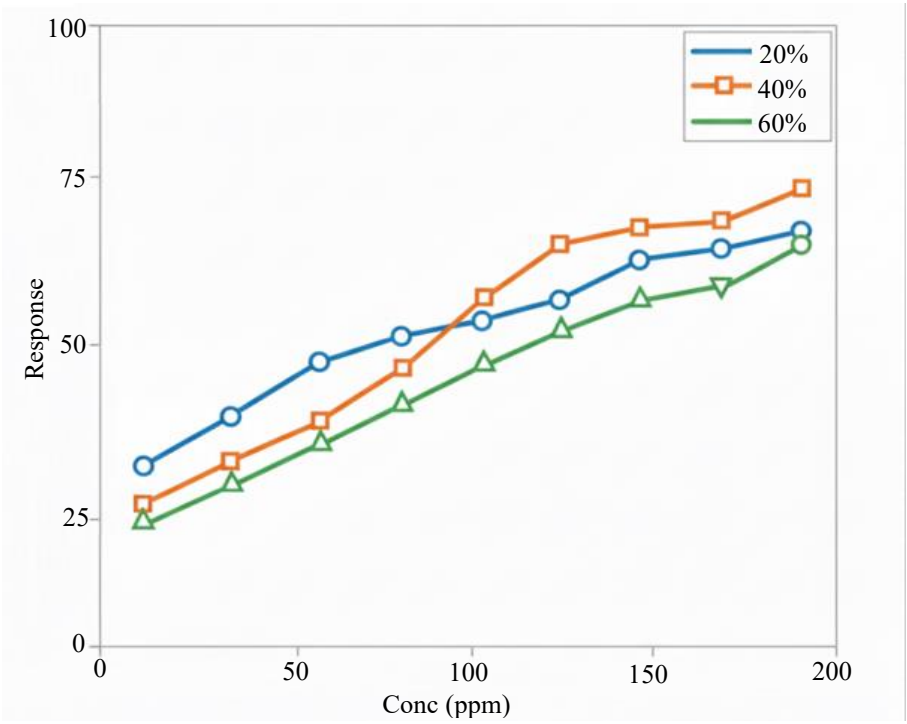

Figure 8. Variation of sensing response with NH_3 concentration (10–200 ppm) for GO/PANI composites.

In the low-concentration range, the sensor response displays an approximately linear dependence on NH_3 concentration, which is consistent with first-order adsorption behavior described by the Langmuir adsorption model. At higher NH_3 concentrations, the rate of response increase gradually diminishes due to the limited availability of active adsorption sites and reduced accessibility of charge-transfer centers. The superior response of the GO/PANI composites compared to pristine GO and PANI sensors is attributed to their optimized microstructure, which promotes efficient gas diffusion, and to strong interfacial coupling between GO sheets and PANI chains that facilitates rapid and effective electron exchange.

The response variation summarized in Figure 8 clearly demonstrates the concentration-dependent sensing behavior of GO/PANI composites, highlighting linear sensitivity at low NH_3 concentrations and saturation trends at higher exposure levels. These characteristics confirm the suitability of the optimized composite for reliable quantitative detection of ammonia in practical sensing applications.

Response and Recovery Time

Response and recovery dynamics are key indicators of the adsorption–desorption kinetics and reversibility of gas–solid interactions in chemiresistive sensors. In this study, the response time is defined as the time required for the sensor resistance to attain 90% of its total change upon exposure to NH_3, whereas the recovery time corresponds to the duration necessary for 90% restoration of the baseline resistance after removal of the target gas. These parameters provide insight into charge-transfer efficiency, diffusion kinetics, and interfacial charge equilibration.

Among all investigated sensing materials, the GO/PANI–40 wt% composite exhibits the most rapid dynamic behavior, with a response time of up to 35 s and a recovery time of up to 50 s, as reflected in the dynamic resistance–time profiles illustrated in Figure 9. The accelerated response is primarily attributed to the presence of a well-percolated GO conductive network, which facilitates fast electron transport and promotes efficient charge redistribution upon NH_3 adsorption. The intimate interfacial contact between GO sheets and PANI chains ensures that charge perturbations induced at adsorption sites are rapidly transmitted throughout the sensing layer.

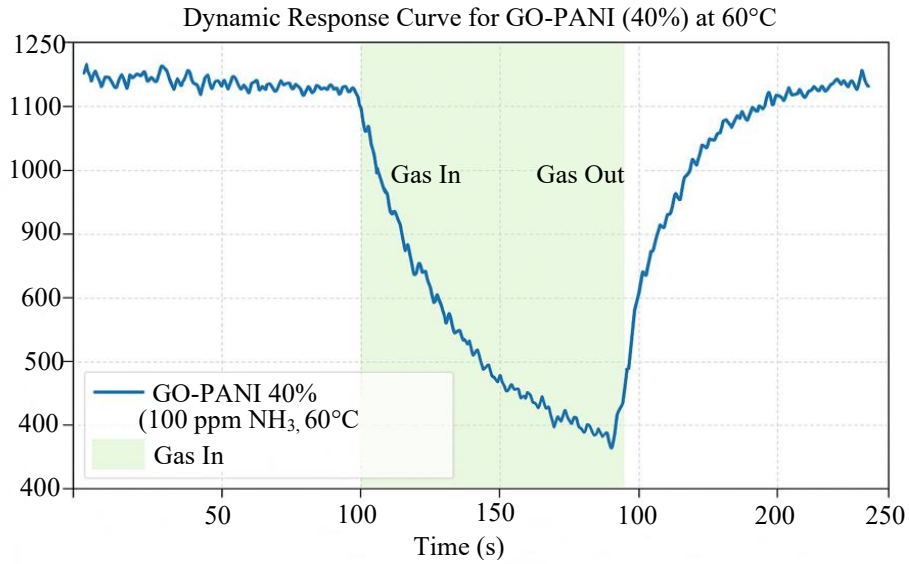

Figure 9. Dynamic response and recovery curves of GO/PANI composite sensors upon repeated NH_3 exposure.

The relatively short recovery time indicates that NH_3 adsorption on the GO/PANI surface is dominated by weak, reversible interactions rather than strong chemisorption. The desorption process is assisted by ambient airflow, which effectively removes NH_3 molecules from adsorption sites and restores the original protonation state of the PANI backbone. In comparison, pristine GO and PANI sensors exhibit slower response–recovery kinetics due to lower carrier mobility, reduced availability of active adsorption sites, and less efficient charge transport pathways. These observations confirm that the optimized GO/PANI interface plays a decisive role in enhancing both adsorption kinetics and reversibility.

Repeatability and Stability

Repeatability and long-term stability are critical parameters for evaluating the practical applicability and reliability of gas sensors under real operating conditions. To assess repeatability, the optimized

GO/PANI–40 wt% sensor was subjected to multiple consecutive NH_3 exposure–desorption cycles at a fixed concentration of 100 ppm. The sensor demonstrates highly consistent response magnitudes over five successive cycles, with negligible variation in baseline resistance or response amplitude, as shown by the cyclic response profiles summarized in Figure 10.

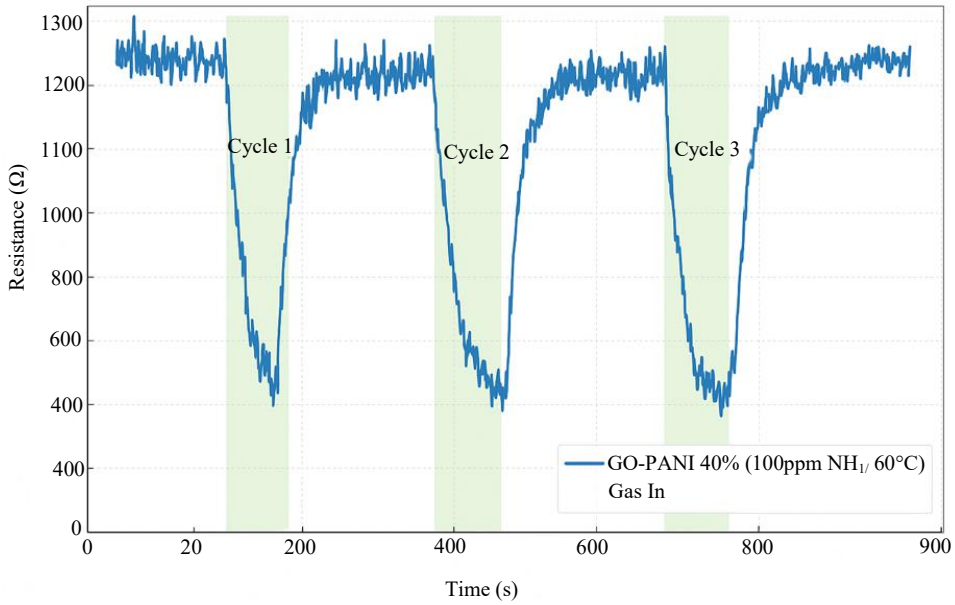

Figure 10. Repeatability and stability performance of GO/PANI-40 composite sensor during multiple exposure–recovery cycles.

The excellent repeatability indicates that the sensing process is fully reversible and that the sensing layer does not undergo permanent structural or chemical changes during repeated gas exposure. This stability is attributed to the robust interfacial bonding between GO sheets and PANI chains, which suppresses polymer chain rearrangement and prevents mechanical degradation during cyclic swelling and contraction.

Long-term operational stability was further evaluated over a period of 30 days under ambient conditions. Throughout the aging period, the GO/PANI–40 sensor retains more than 95% of its initial sensing response without noticeable baseline drift or signal degradation. This exceptional stability arises from the chemical robustness of GO, which resists oxidation and structural collapse, and from the stabilized emeraldine salt form of PANI, which maintains its conductive state over prolonged operation. The synergistic integration of GO and PANI, therefore, ensures sustained electrical conductivity, structural integrity, and sensing reliability over extended timescales.

Effect of Gas Concentration on Resistance

To further elucidate the sensing mechanism, the variation of sensor resistance as a function of NH_3 concentration was systematically investigated. Upon exposure to increasing NH_3 concentrations, the sensor resistance increases progressively, reflecting deprotonation of the PANI backbone and a corresponding decrease in hole carrier concentration. This behavior is characteristic of p-type conducting polymers interacting with electron-donating reducing gases.

Among the tested sensors, the GO/PANI–40 wt% composite exhibits the steepest resistance–concentration slope, indicating superior charge sensitivity and higher surface reactivity. The resistance variation trends shown in Figure 11 highlight the enhanced ability of this composite to transduce surface adsorption events into measurable electrical signals. At low NH_3 concentrations, the nearly linear dependence of resistance on gas concentration suggests uniform adsorption and efficient charge transfer across the GO–PANI interface, consistent with Langmuir-type adsorption behavior.

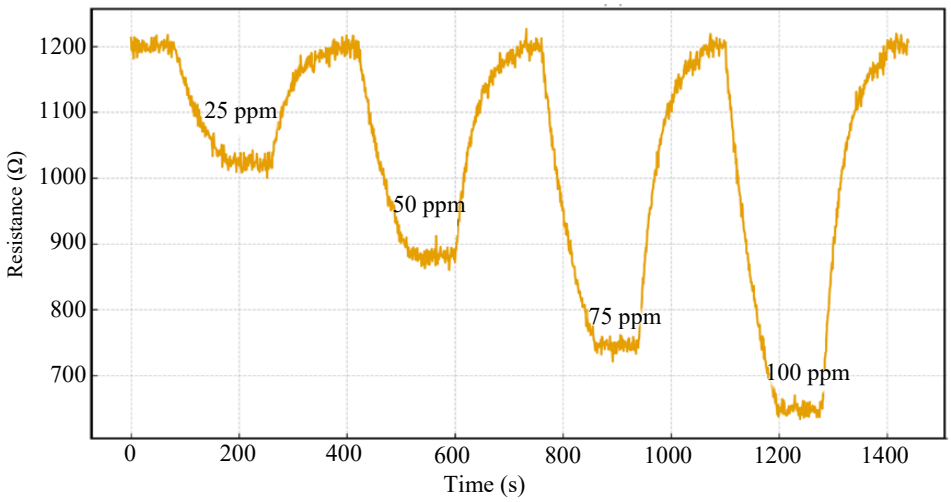

Figure 11. Multi-concentration NH_3 pulse response (25–100 ppm) of GO–PANI (40%) nanocomposite at 60°C.

At higher NH_3 concentrations, the resistance response gradually approaches saturation due to the exhaustion of available adsorption sites and limited accessibility of active charge-transfer centers. Importantly, the resistance returns to its initial value upon gas removal, confirming the reversibility and dynamic stability of the sensing process. The observed behavior demonstrates that the hybrid interface effectively combines the high carrier mobility and large surface area of GO with the chemical sensitivity of PANI, resulting in an efficient and stable sensing platform.

Several recent studies have reported gas-sensing performances comparable to the present GO/PANI system, highlighting the effectiveness of graphene–polyaniline hybrid architectures for room-temperature NH_3 detection. Yang et al. [20] reported a highly sensitive NH_3 sensor based on a polyaniline/laser-induced graphene (PANI/LIG) composite operating at room temperature, demonstrating fast response and recovery characteristics attributed to the synergistic combination of conductive graphene networks and the protonated PANI backbone. Their results emphasize the role of graphene-assisted charge transport in accelerating sensing kinetics.

Similarly, Liang et al. [21] developed a multichannel PSS-functionalized graphene/PANI network for NH_3 sensing, which exhibited enhanced sensitivity and long-term stability at ambient conditions. The improved performance was associated with the formation of interconnected graphene pathways and strong interfacial coupling with PANI, facilitating efficient charge transfer and selective adsorption of NH_3 molecules.

In another related study, Wang et al. [22] reported a flexible, substrate-free NH_3 sensor based on PANI-coated reduced graphene oxide (rGO) functionalized fibers. The sensor showed excellent selectivity, low detection limits, and reliable room-temperature operation, which were attributed to the high surface area of rGO and the strong acid–base interaction between NH_3 and PANI.

In comparison with these reported systems, the present GO/PANI composite sensor exhibits comparable room-temperature performance with fast response–recovery dynamics, good selectivity, and excellent stability. The consistent trends across these studies confirm that strong interfacial interactions between graphene-based materials and polyaniline, combined with optimized microstructure, are key factors governing high-performance NH_3 sensing.

The comprehensive gas-sensing investigation clearly establishes that the GO/PANI–40 wt% composite offers the most favourable combination of sensitivity, selectivity, response–recovery kinetics, repeatability, and long-term stability. The enhanced sensing performance originates from synergistic effects between GO

and PANI, including optimized interfacial charge transfer, increased adsorption capacity, improved electrical conductivity, and structural robustness [23]. These findings highlight the suitability of GO/PANI composites for reliable room-temperature NH_3 detection and suggest that the sensing platform can be extended to other volatile analytes through rational surface modification and compositional tuning.

CONCLUSION

GO, PANI, and GO/PANI composites with different PANI loadings were successfully synthesized via in-situ oxidative polymerization and systematically investigated. Structural and spectroscopic analyses confirmed strong interfacial coupling and partial intercalation of PANI within GO layers, accompanied by a well-developed interconnected morphology, most pronounced for the GO/PANI–40 composition. Optical studies revealed enhanced electronic delocalization with increasing PANI content, reflected by a progressive reduction in the optical band gap. Gas-sensing measurements demonstrated that GO/PANI composites exhibit superior room-temperature NH_3 sensing performance compared to pristine GO and PANI, with GO/PANI–40 delivering the most balanced combination of sensitivity, selectivity, rapid response–recovery, and operational stability. These findings underline the critical role of interfacial engineering in tailoring the functional properties of GO/PANI hybrids and support their potential for advanced room-temperature gas-sensing applications.

REFERENCES

1. Modak PR. Synthesis, optical study and band gap energy of PANI/GNS nanocomposite. AIP Adv. 2024;14(2):020015.
2. Almasi MJ. Band gap study of polyaniline and polyaniline/MWNT nanocomposites with in situ polymerization method. Compos B Eng. 2016;(9):63–8.
3. Ahuja P. Hierarchically grown NiO-decorated polyaniline-reduced graphene oxide for enhanced light absorption. ACS Omega. 2018;3(1):876–85.
4. Mohammed HY, Al-Aws AS, Ahmad M. Selective and sensitive chemiresistive sensors based on GO/PANI nanocomposite: Improved performance for NH3 detection. Sens Actuators A Phys. 2022;(333):113274.
5. Hadano FS, Gavim AEX, Stefanelo JC, Gusso SL, Macedo AG, Rodrigues PC, et al. NH3 sensor based on rGOPANI composite with improved response and recovery. J Sens. 2021;15:4947.
6. Chang J, Zhang X, Wang Z, Li C, Hu Q, Gao J, et al. Polyaniline-reduced graphene oxide nanosheets for room-temperature ammonia gas sensing. ACS Appl Nano Mater. 2021;4(5):5026–35.
7. Mahmoud AA, Khafagy RM, Ibrahim MA. Investigating the electronic properties of PANI/graphene/PVDF/PTFE nanocomposite. Opt Quantum Electron. 2024;56(4):666.
8. Esmaeili C, Ashtiani S, Regmi C, Laposa A, Voves J, Kroutil J, et al. Preparation and characterisation of NH3 gas sensor based on PANI/Fe-doped CeO2 nanocomposite. Heliyon. 2024;10(15).
9. Tawade AK, Patil VL, Patil SC, Tayade SN, Pawar KK, Kumar PK, et al. Reduced graphene oxide-polyaniline hybrid nanocomposite for selective sensing of ammonia gas at room temperature. Ceram Int. 2024;50(8):13196–13207.
10. Verma A, Kumar T. Ag/Cu doped polyaniline hybrid nanocomposite-based novel gas sensor for enhanced ammonia sensing at room temperature. RSC Adv. 2024;14(60):34789–97.
11. Aalam SM, Farooq A, Sarvar M, Bhat MN, Tomar M, Raza MMH, et al. To study the performance of polyaniline-based copper and carbon-nanotube (PANI@ Cu@ CNT) nanocomposite for harmful NH3 gas sensing. Sci Rep. 2025;15(1):26886.
12. Gaikwad G, Patil P, Patil D, Naik J. Synthesis and evaluation of gas sensing properties of PANI based graphene oxide nanocomposites. Mater Sci Eng B. 2017;218:14–22.
13. Aghaei SM, Monshi MM, Torres I, Calizo I. Adsorption and dissociation of toxic gas molecules on graphene-like BC3: A search for highly sensitive molecular sensors and catalysts. arXiv preprint arXiv:1706.00774. 2017.
14. Shaban M, Rabia M, Abd El-Sayed AM, Ahmed A, Sayed S. Photocatalytic properties of PbS/graphene oxide/polyaniline electrode for hydrogen generation. Sci Rep. 2017;7(1):14100.

15. Saçak S, Cankurtaran H, Ugraskan V. Synergistic electrocatalytic effect of carbon paste electrode modified with boron phosphate–polyaniline composite on voltammetric determination of paracetamol and ascorbic acid. J Mater Sci Mater Electron. 2025;36(23):1450.
16. Al-Sulami AI, Elamin NY, Aldosari E, Farea MO, Alzahrani SS, Al-Harthi AM, et al. Tunable band gap and ionic conductivity in PMMA and PANI blend with WO_3 nanocomposites for optoelectronics and energy storage devices. Sci Rep. 2025;15(1):34543.
17. Arthisree D, Madhuri W. Optically active polymer nanocomposite composed of polyaniline, polyacrylonitrile and green-synthesized graphene quantum dot for supercapacitor application. Int J Hydrogen Energy. 2020 Mar 20;45(16):9317–27.
18. Mahmoud AA, Khafagy RM, Ibrahim MA. Investigating the electronic properties of PANI/graphene/PVDF/PTFE nanocomposite. Opt Quantum Electron. 2024;56:666. doi: 10.1007/s11082-024-06320-y.
19. Kumawat RL, Jena MK, Pathak B. Black arsenic as an optimum gas sensor: vdW corrected density functional theory calculations. arXiv preprint arXiv:2003.13411. 2020 Mar 22.
20. Yang L, Mao L, Du S, Wang Z, Fu W, Yao C, et al. Highly sensitive and fast response/recovery ammonia sensor based on PANI/LIG at room temperature. Sens Actuators B Chem. 2025 Aug 15;437:137710.
21. Liang H, Zhu Y, Zhao Z, Tang Z, Niu Y, Zhang D, et al. Enhanced room temperature ammonia gas sensing based on a multichannel PSS-functionalized graphene/PANI network. Analyst. 2025 Feb 10;150(4):669–79.
22. Wang Z, Ni L, Zhang X, Feng L. A novel flexible substrate-free NH3 sensing membrane based on PANI covered rGO functionalized fiber. Sens Actuators B Chem. 2023 Apr 1;380:133307.
23. Gaikwad G, Patil P, Patil D, Naik J. Synthesis and evaluation of gas sensing properties of PANI based graphene oxide nanocomposites. Mater Sci Eng B. 2017 Apr 1;218:14–22.

